

Pearcey vortex beam dynamics through atmospheric turbulence

Shakti Singh¹, Sanjay Kumar Mishra², Akhilesh Kumar Mishra^{1,*}

¹Department of Physics, Indian Institute of Technology Roorkee, Roorkee-247667, India

²Photonics Division, Instruments Research and Development Establishment, Dehradun-248008, India

*Corresponding author: akhilesh.mishra@ph.iitr.ac.in

Abstract: The subject area of free space optical communication (FSO) with optical beam carrying orbital angular momentum (OAM) has attracted a great deal of research attention since last two decades. In this paper, we present a numerical investigation of the propagation characteristics of Pearcey vortex beam (PVB) through the atmospheric turbulence. The study details on both moderate as well as strong atmospheric turbulences. Von Karman model has been relied on to model random phase screen. It has been observed that in moderate turbulence PVB preserved its singularity while in strong turbulence, for shorter distance PVB preserves its singularity characteristics whereas at larger distance the singularity is lost. We have also calculated the apertured average scintillation and noticed that PVB with truncation factor $b = 0.1$ performs better in stronger turbulence while in moderate turbulence, the apertured average scintillation performs better only for relatively larger truncation factor. Further, we have compared the apertured average SI of PVB and Laguerre Gauss (LG) beam and found that in strong turbulence PVB exhibits better SI compared to LG beam. Even in moderate turbulence, PVB outperforms LB beams for short distances.

1. Introduction

Optical beam propagation through atmosphere has drawn considerable attention due to its applications in many areas like free space optical communication (FSO) both classical and quantum [1], remote sensing [2], laser guided defence system and imaging [3] to name a few. Turbulence strongly affects the refractive index of the atmosphere and therefore it gives unexpected consequences in the optical beams such as intensity fluctuation, beam wandering, decrease in spatial coherence and loss of optical power [4-6]. Intensity fluctuation in optical beams is characterised by a physical quantity called, scintillation index (SI) [7]. The scintillation results due to the distortion in the wavefront of optical beam by turbulence. In FSO the SI of an optical beam at the detector end should be minimum [8]. An optical beam that has ability to resist the turbulence strongly is preferred for FSO. A nondiffracting and self-healing beams such as Bessel [9] and Airy beams [10-11] have the potential to overcome turbulence induced deformations. Due to rigorous stochastic nature of atmospheric turbulence, analytical solution of the of Helmholtz equation exists only for limited number of optical beams. These solutions are restricted to the lower order statistics. Therefore, numerical modelling becomes essential tool for understanding the nature the of complex optical through the atmospheric turbulence.

Scintillation of the optical beams after propagating through the turbulence have been studied for scalar beams such as Laguerre-Gauss beam [12], Bessel beam [13], Airy vortex beam [14], cos and cosh-Gaussian beam [15], elliptical vortex beam [16] and flat top beam [17]. Vortex beam is a special kind of beam which possesses undefined phase at the centre of the beam [18-20]. To overcome the turbulence induced intensity fluctuations many techniques have been proposed. Coherence of optical beams also affect the SI and it has already been shown that partially coherent beams have lower scintillation compared to the fully coherent beams [21-23]. A coherent beam with non-uniform polarization also show lower SI compared to the

coherent beam with uniform polarization [24-28]. Beam arrays, which are constituents of spatially separated beamlets, have been used for reducing the scintillation by adjusting the spatial separation among the beamlets [29-30]. A deviation in the spatial separation of beamlets causes significant increase in the SI. These days there are growing interest in free space optical communication and remote sensing using optical vortex beams. Vortex beam carry orbital angular momentum (OAM), which can be multiplexed to encode information data for transmission in FSO [31]. Vortex beam propagation through atmospheric turbulence has also been explored from the perspective of quantum communication and quantum entanglement [32-33].

In the last decade abruptly autofocusing (AAF) beams have emerged as an interesting class of beams that exhibit unprecedented properties like nondiffracting and self-healing [10]. AAF beam have applications in micromanipulation and biomedical treatment. Circular airy beam was the first AAF beam which was introduced in 2010. This auto focussing behaviour of such beams owes its origin in the optical field structure [6-7]. Circular Pearcey beam is another example of AAF beams, whose analytical expression comes from transforming the Pearcey function to the cylindrical coordinate [34-36]. Optical vortex when assigned to any optical beam modifies its characteristics extensively. AAF beams superimposed with optical vortices have also been explored extensively in the literature. In particular, propagation characteristics of AAF airy beam with optical vortices has recently been investigated in ref [30-31]. AAF Pearcey beams have also been studied experimentally long back[37]. During propagation in atmospheric turbulence AAF beams balance the beam wander and spreading of beams, which in turn help in reducing the crosstalk talk, SI and bit error rates which ultimately improves the FSO link[8].

In the present work, we numerically report the propagation characteristics of Pearcey vortex beam (PVB) through the atmospheric turbulence. The propagation of PVB through atmospheric turbulence is modelled by Von Karman spectrum with FFT method. The paper is arranged as follows- in section (2) we have discussed the numerical model. In section (3) we have discussed the profile of PVB and the numerical simulation parameters. Section (4) first discusses the intensity variation of PVB in free space and turbulent atmosphere with varying strength of turbulence. Next, the variation of apertured average SI with propagation distance for different topological charge and truncation factor are elaborated. Section (5) concludes the work.

2. Numerical Model

Optical beam propagation through any medium is modelled by Helmholtz equation. But in turbulent atmosphere due random nature of refractive index, the propagation is modelled by stochastic Helmholtz equation. Randomly varying refractive index is characterized by power spectral density (PSD). PSD describes the statistical distribution of the number and size of turbulent eddies [4]. Optical beam propagation through atmospheric turbulence is modelled by multiple phase screen method [38-39]. In this method we treat the turbulent atmosphere as a collection of thin random phase screens placed along the propagation direction with equal interval of free space. Randomly varying phase imposed on these phase screens enables them to mimics atmospheric turbulence. Different types PSD have been proposed for modelling the

propagation of optical beam through atmospheric turbulence. The widely employed one is Kolmogorov spectrum whose mathematical expression is written as [39]

$$\phi_n(\kappa) = 0.033c_n^2\kappa^{-11/3} \text{ for } \frac{2\pi}{L_0} < \kappa < \frac{2\pi}{l_0} \quad (1)$$

In above PSD in the limit $\kappa \rightarrow 0$, it contain a singularity in the form of non-integrable pole. To overcome this, another PSD model called Tatarskii spectrum was proposed, which is given by [39]

$$\phi_n(\kappa) = 0.033c_n^2\kappa^{-11/3} \exp\left(\frac{-\kappa^2}{\kappa_m^2}\right) \text{ for } \kappa > \frac{2\pi}{L_0} \quad (2)$$

where $\kappa_m = \frac{5.92}{L_0}$. This spectrum also contains a singularity when $L_0 \rightarrow \infty$. Another important PSD called von Kármán spectrum has also been introduce, which is expressed by

$$\phi_n(\kappa) = 0.033c_n^2(\kappa^2 + \kappa_0^2)^{-11/6} \text{ for } 0 \leq \kappa \ll \frac{2\pi}{l_0} \quad (3)$$

For taking the entire range of κ a modified Von Karman type PSD was proposed for refractive index fluctuation 3modelling of the atmosphere. Its expression is given by [12]

$$\phi_n(\kappa) = 0.033c_n^2(\kappa^2 + \kappa_0^2)^{-11/6} \exp\left(\frac{-\kappa^2}{\kappa_m^2}\right) \quad (4)$$

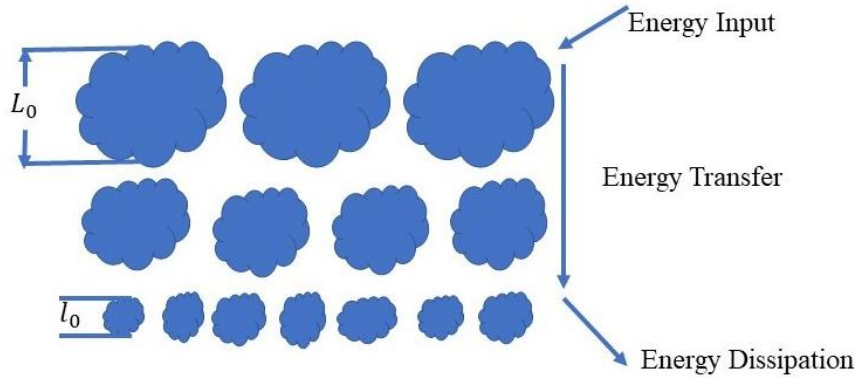


Figure 1. Energy cascade theory of turbulence

where c_n^2 represents the refractive index structure constant that represents the strength of atmospheric turbulence. The typical value of c_n^2 varies from $10^{-17}m^{-2/3}$ to $10^{-12}m^{-2/3}$ [12]. κ represents the magnitude of three-dimensional spatial frequency vector in cartesian coordinate. In the above equation, $\kappa_0 = \frac{2\pi}{L_0}$ and $\kappa_m = \frac{5.92}{l_0}$, where L_0 represents the outer scale and l_0 represents the inner scale of the atmospheric turbulence. In turbulent atmosphere, unstable air masses due to influence of inner forces break up into smaller turbulent eddies to form a continuum of eddy size for transfer of energy from outer scale L_0 to inner scale l_0 . Atmosphere behaves like isotropic and homogeneous only when the size of turbulent eddies lies between inner scale l_0 and outer scale L_0 . The typical magnitude of inner scale is of order milli-meter and outer scale is of order meter near the ground and their values increases as we move upward. The required number of random phase screens depends upon the propagation

distance and strength of the turbulence. In this numerical investigation we have taken $l_0 = 1\text{ cm}$ and $L_0 = 3\text{ m}$ and we have used 20 random phase screens at equal interval of the total propagation distance, which is 2 km in our numerical experiment.

The random phase screen is generated by considering a $N \times N$ array of complex Gaussian random number $a + ib$ and then this complex number is multiplied with the square root of phase spectrum. The phase spectrum and power spectrum are related and are expressed as [12]

$$\phi_\theta(\kappa) = 2\pi k^2 \delta z \phi_n(\kappa) \quad (5)$$

where k is the wavevector, δz is the distance between the phase screens. Now we multiply the complex Gaussian random number by $\Delta_K^{-1} \sqrt{\phi_\theta(\kappa)}$, where $\Delta_K^{-1} = 2\pi/N\Delta$, N is the number of sampling point and Δ is the spatial sampling interval. The result is then inverse Fourier transformed to get the random phase $\theta_1 + i\theta_2$. The generation of phase screen by above mentioned method for propagation through the atmospheric turbulence is called FFT method. Throughout our numerical investigation we have chosen θ_1 as random phase screen. To validate our numerical model, we have first generated the results of published paper in references [8-10]. Propagation chart (algo) of optical beam through atmospheric turbulence is illustrated in the figure (2). First, we propagate the optical beam up to a distance δz under diffraction by employing angular spectrum method where 2D Fourier transform of the optical field is multiplied with the free space transfer function, whose expression is given by the equation (6). The resultant optical field illuminates the phase screen, and this process continues until the final distance is reached.

$$A(f_x, f_y) = \exp(i\delta z \sqrt{k^2 - 4\pi^2(f_x^2 + f_y^2)}) \quad (6)$$

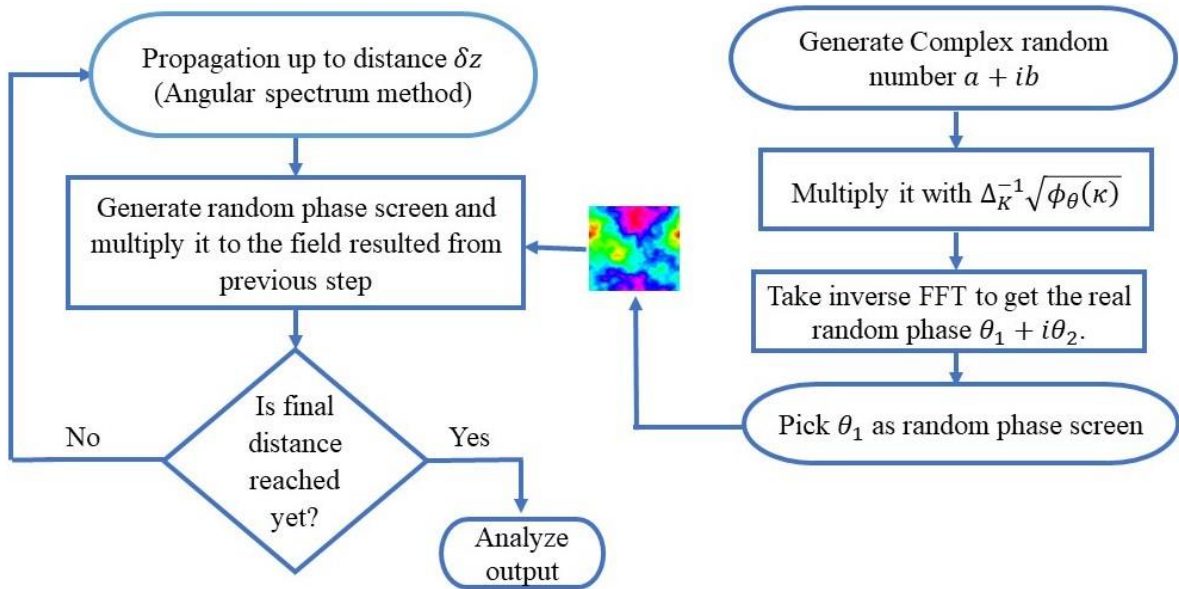


Figure 2. Propagation flow chart used in our numerical model

3. Numerical simulation Parameters

In our numerical investigation, we have studied the propagation of PVB through atmospheric turbulence whose input complex field distribution is given by

$$E(r, \phi, 0) = Pe\left(\frac{-r}{w_0}, \zeta_0\right) \exp\left[b\left(\frac{-r}{w_0}\right)\right] \exp(il\phi) \quad (7)$$

where Pe is the Pearcey function, which is defined by an integral representation as given by

$$Pe(x, y) = \int_{-\infty}^{\infty} \exp(is^4 + is^2x + isy) ds \quad (8)$$

here x and y are dimensionless transverse variables. In equation (7), w_0 is the width of the primary ring of the beam, l is the topological charge of PVB, b is truncation factor and ϕ is the azimuth angle ζ_0 denotes a constant. In our simulation, we have taken $w_0 = 3 \text{ cm}$, wavelength $\lambda = 2 \mu\text{m}$, $l_0 = 1 \text{ cm}$, $L_0 = 3 \text{ m}$, $N = 500$, $\zeta_0 = 0$ and rest of the parameters are specified in the respective figure captions [14]. We have propagated our optical beam up to 2 Km and have used 20 random phase screens at an interval of 100 m . Moreover, we have considered 500 independent realizations to provide the sufficient statistics for the calculation of average irradiance and scintillation index.

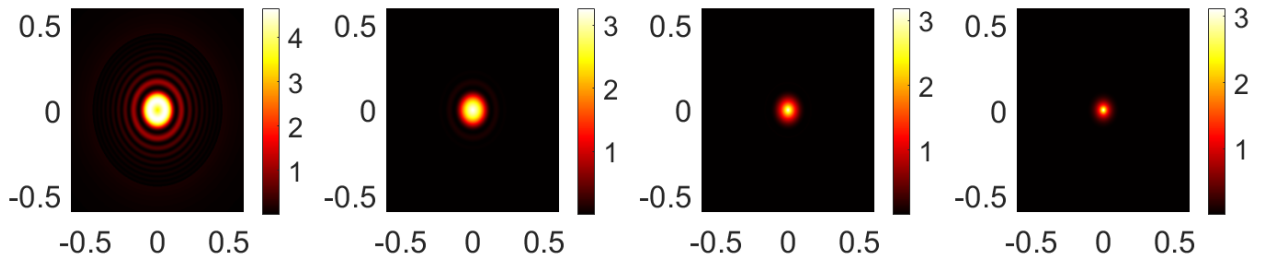


Figure 3. Input beam intensity profile of PVB with $l=1$ for different values of truncation factor, (a) $b=0.1$, (b) $b=0.3$, (c) $b=0.5$ and $b=0.7$ in (d).

4. Results and Discussion

4.1 Propagation effects in atmospheric turbulence

For understanding the dynamics of PVB in the atmosphere we, in figure 4, have plotted the evolution of intensity profiles of PVB in both moderate and strong turbulences. The first row in figure 2 shows the evolution of PVB in free space without turbulence, wherein the optical beam shows self-focusing property. Second row shows the evolution in moderate turbulence ($c_n^2 = 10^{-14}$), wherein we observe that although the PVB maintains its singular characteristic, its self-focussing strength has got weakened. The singularities characteristic as preserved by PVB is due its self-healing properties. For strong turbulence ($c_n^2 = 10^{-12}$), as depicted in the third row, we observe that despite the strong turbulence PVB try to preserve its singularity characteristic up to 500m but on furthering the propagation distance the PVB losses its typical singular behaviour. We also observe that in strong turbulence PVB do not preserve its self-focussing properties. For smaller distances, the effect of atmospheric turbulence is very moderate but on increasing the distance the beam gets distorted heavily and irreparably.

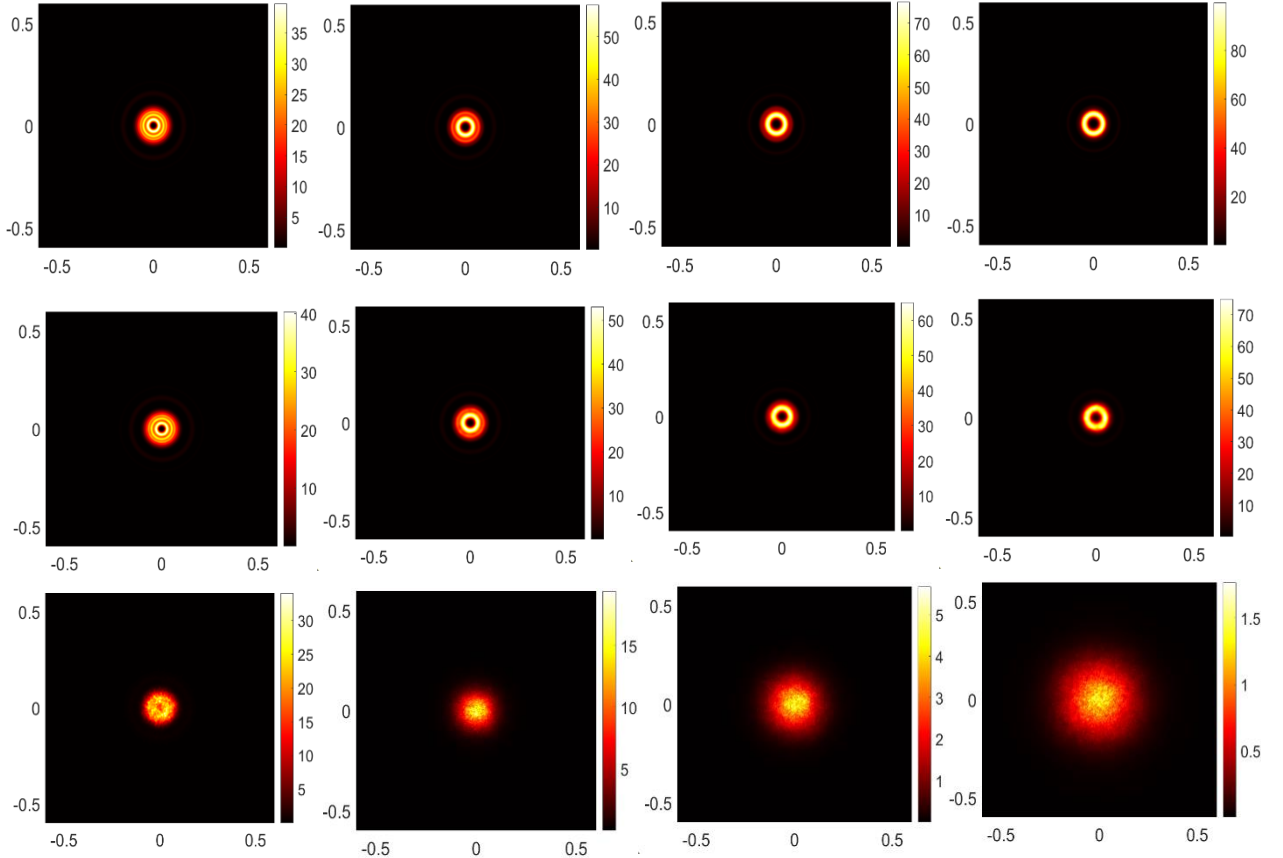


Figure 4. Transverse intensity profile evolution of PVB for $l = 1$ and $b = 0.1$ in free space without turbulence (1st row), with moderate turbulence ($C_n^2 = 10^{-14}$) (2nd row) and with strong turbulence ($C_n^2 = 10^{-12}$) (3rd row). The four columns represent the cross-sectional intensities at $z=500$ m, $z=1000$ m, $z=1500$ m and at $z=2000$ m respectively.

4.2 Apertured average scintillation in atmospheric turbulence

The optical beam quality through atmospheric turbulence is characterized by measuring the on-axis SI. The SI at a transverse position (x, y) in detector plane is defined by [39]

$$\sigma_I^2(x, y, z) = \frac{\langle (I(x, y, z))^2 \rangle}{\langle I(x, y, z) \rangle^2} - 1 \quad (9)$$

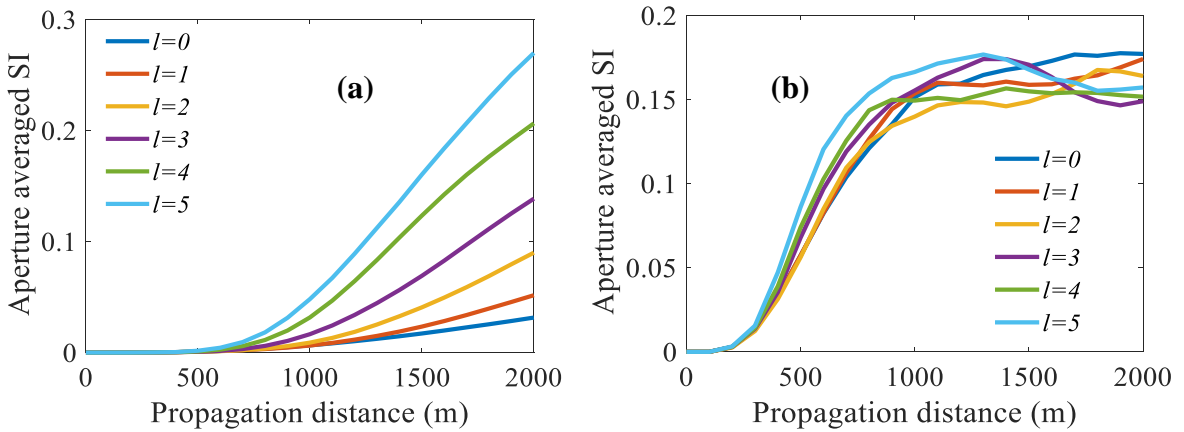


Figure 5. Apertured average SI for PVB with propagation distance for moderate and strong turbulence parameters, (a) $C_n^2 = 10^{-14}m^{-2/3}$ (b) $C_n^2 = 10^{-12}m^{-2/3}$.

where I is the irradiance of the optical beam and $\langle \rangle$ represents the ensemble average. $\langle I(x, y, z) \rangle$ is obtained by summing the independent realization and then dividing the outcome by total number of realizations. Since the detector, we use for measuring the SI in experiments, have finite aperture size and therefore it gives us aperture average effects. To align our numerical results with the experimental measurements, we calculate the aperture-averaged scintillation index, which is given by [10]

$$S(z) = \frac{\langle (\int_{-R}^R \int_{-R}^R I(x, y, z) dx dy)^2 \rangle}{\langle \int_{-R}^R \int_{-R}^R I(x, y, z) dx dy \rangle^2} - 1 \quad (10)$$

Moreover, the apertured average scintillation is more stable than usually calculated on-axis SI therefore our results are more realistic. In figure 5 we have shown the apertured average SI for PVB. Figure 5(a) represents the SI in moderate turbulence for different topological charge l . It is noticed that with propagation the SI increases. On increasing the value of l the SI of the beam becomes larger because larger l makes outer wall of PVB thinner and this increases the SI. In strong turbulence, as depicted in figure 5(b), SI peaks at a particular distance of propagation and on further propagation it decreases because of auto compensation effects [16].

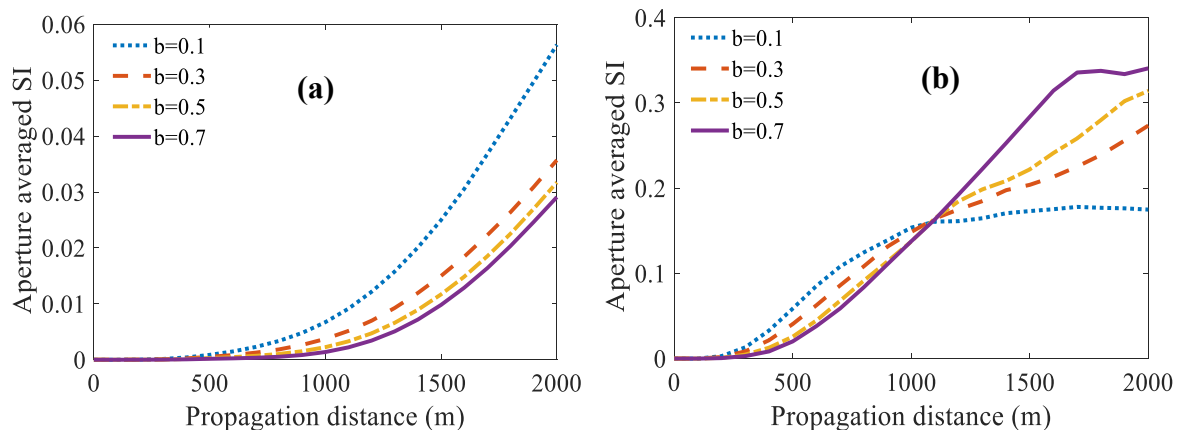


Figure 6. Apertured average scintillation index for $l = 1$ and different value of truncation factor and truncation parameters: (a) $C_n^2 = 10^{-14}m^{-2/3}$ (b) $C_n^2 = 10^{-12}m^{-2/3}$

In figure 6, we have studied the apertured average SI of PVB for different values of truncation factor. It is observed that the apertured average SI increases with propagation distance in moderate atmospheric turbulence. On increasing the value of truncation factor, SI reduces. In media with stronger turbulence (see figure 6 (b)), apertured average SI evolution becomes complex. With increasing truncation factor the beam loses its self-healing capability and once the parameter is chosen to be very large the beam ceases to heal itself and therefore SI starts to increase with propagation. Such as observation can easily be understood as with the increase of the truncation factor the loses its shape and therefore its typical characteristics.

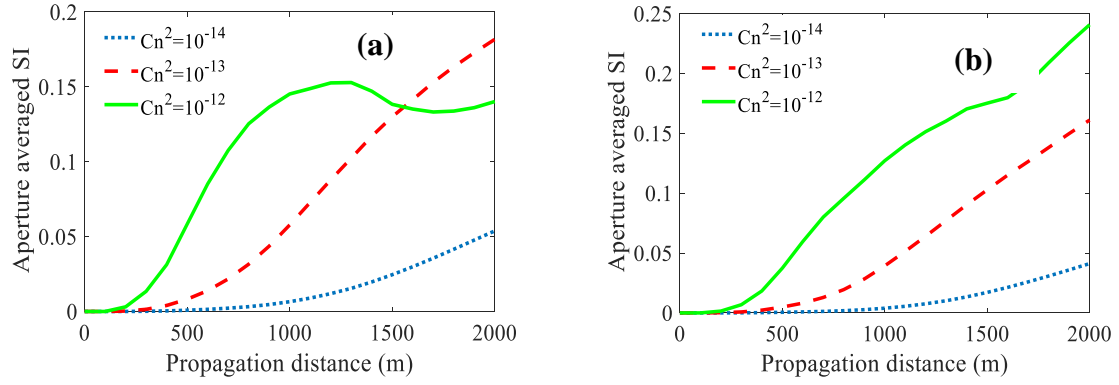


Figure 7. Variation of apertured averaged SI with propagation for beam with $l=1$, (a) $b = 0.1$ and (b) $b = 0.3$ for different levels of turbulence.

In figure 7, we vary the level of atmospheric turbulence and calculate the SI with propagation for $b = 0.1$ in fig 7(a) and $b = 0.3$ in fig 7(b). We found that for stronger turbulence SI rises up even at lower distances. Figure 7(b) depicts that stronger b deteriorates SI.

4.3 Scintillation of Laguerre Gauss beam and PVB

In this section we have compared the apertured average SI of Laguerre Gauss (LG) beam and PVB and found that in strong turbulence (see fig. 8 (c)) PVB exhibits better SI compared to LG beam. In weak and moderate turbulence (see fig. 8 (a) and (b)), LG beam has better SI compared to PVB beams. Because of multiple thinner rings PVB exhibits high SI at smaller distance as compare to that in LG beam as shown in Figure 8(c). However, at larger distance, due to relatively stronger self-healing effect, PVB performs better. This is also clearly depicted in the figure that PVB has better self-healing property in strong turbulence and that leads to smaller SI in stronger turbulence. Thus we can conclude that in stronger turbulence, PVB performs better as compare to LG beam.

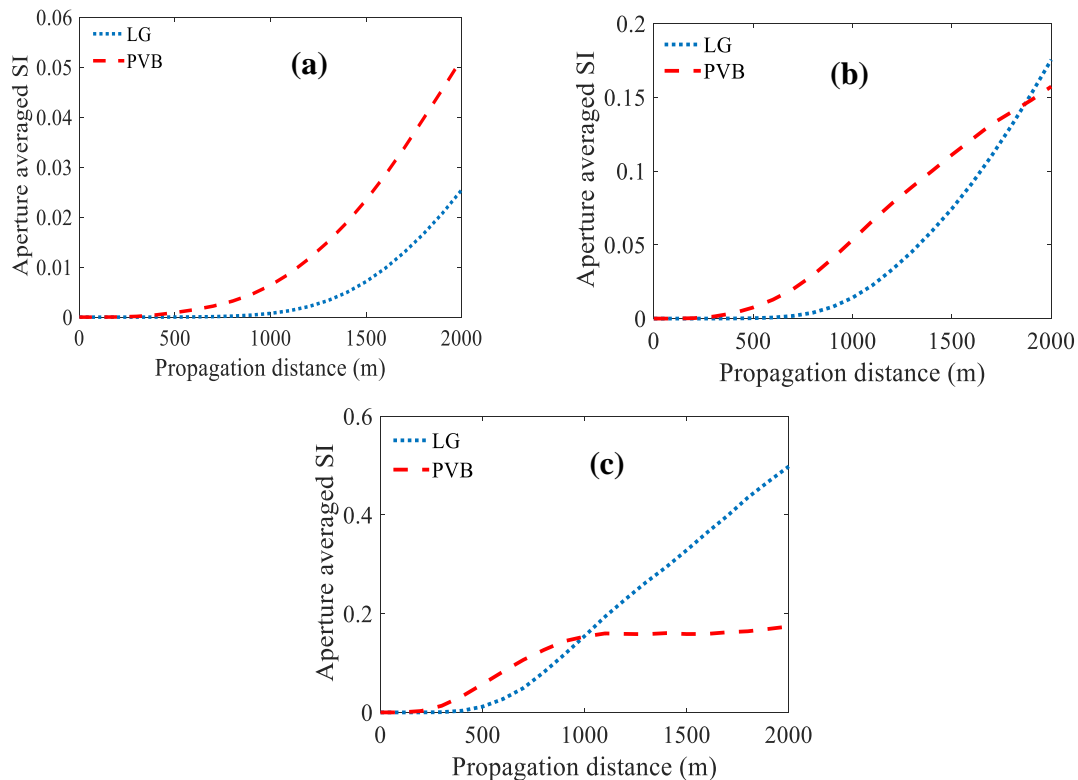


Figure. 8. Apertured average scintillation index for $l = 1$ and in case of PVB $b = 0.1$ of LG and PVB beam.: (a) $C_n^2 = 10^{-14} m^{-2/3}$ (b) $C_n^2 = 10^{-13} m^{-2/3}$ (c) $C_n^2 = 10^{-12} m^{-2/3}$.

5. Conclusion

In summary we have investigated the propagation dynamics of PVB through atmospheric turbulence for different topological charges and truncation factors. We have studied the apertured average SI of PVB and found that on increasing the value of topological charge l , SI increases in moderate turbulence but shows saturation effect in strong atmospheric turbulence. Further, it has been observed that on increasing the value of truncation factor in moderate turbulence the value of apertured average SI decrease and in strong turbulence the saturation is lost. In addition, the apertured average SI is found to increase with increasing value of the truncation factor. Moreover, PVB is found to outperform LG beam in strong turbulence.

We believe that our study may find application in the FSO, remote sensing and space communication for better performance.

Acknowledgement

SS wishes to acknowledge the University Grant Commission (UGC), India for the financial support. AKM acknowledges the Faculty Initiation Grant (FIG) provided by IIT Roorkee, India.

References:

1. A. E. Willner, K. Pang et al., "Orbital angular momentum of light for communications" *Appl. Phys. Rev.* **8** 041312-68 2021
2. B. M. Welsh and S. C. Koeffler, "Remote sensing of atmospheric turbulence and transverse winds from wave-front slope measurements from crossed optical paths" *Appl. Opt.* **33**(21), 4880-4888, 1994
3. D. A. Hope et al., "High-resolution speckle imaging through strong atmospheric turbulence" *Opt. Express* **24** (11), 12116-12129, 2016
4. O. Korotkova and E. Wolf, "Beam criterion for atmospheric propagation," *Opt. Lett.* **32**(15), 2137–2139 (2007).
5. X. Ji, H. T. Eyyubođlu, and Y. Baykal, "Influence of turbulence on the effective radius of curvature of radial Gaussian array beams," *Opt. Express* **18**(7), 6922–6928 (2010).
6. X. Ji, H. T. Eyyubođlu, and Y. Baykal, "Influence of turbulence on the effective radius of curvature of radial Gaussian array beams," *Opt. Express* **18**(7), 6922–6928 (2010).
7. K. Khare, P. Lochab and P. Senthilkumaran, "Orbital Angular Momentum States of Light Propagation through atmospheric turbulence" IOP Publishing (2020)
8. J. Durnin, "Exact solutions for nondiffracting beams. I. The scalar theory," *J. Opt. Soc. Am. A* **4**(4), 651–654 (1987).
9. N. K. Efremidis and D. N. Christodoulides, "Abruptly autofocusing waves," *Opt. Lett.* **35**(23), 4045–4047 (2010).

10. D. G. Papazoglou, N. K. Efremidis, D. N. Christodoulides, and S. Tzortzakis, "Observation of abruptly autofocusing waves," *Opt. Lett.* **36**(10), 1842–1844 (2011).
11. M. Abtahi et al., "Suppression of Turbulence-Induced Scintillation in Free-Space Optical Communication Systems Using Saturated Optical Amplifiers" *J. Light. Technol.* **24**(12), 4966-4973, 2006
12. W. Cheng, J. W. Haus, and Q. Zhan, "Propagation of vector vortex beams through a turbulent atmosphere," *Opt. Express*, **17**(20), 17829-36, (2009)
13. H. T. Eyyuboglu, "Propagation of higher order Bessel-Gaussian beams in turbulence," *Appl. Phys. B* **88**(2), 259–265 (2007).
14. K. Yang, S. Tang, X. Yang, and R. Zhang, "Propagation characteristics of a ring Airy vortex beam in slant atmospheric turbulence" *J. Opt. Soc. Am. B* **38**(5), 1510-1517 (2021).
15. H. T. Eyyuboglu, "Annular, cosh, and cos Gaussian beams in strong turbulence," *Appl. Phys. B* **103**, 763–769 (2011).
16. X. Liu and J. Pu, "Investigation on the scintillation reduction of elliptical vortex beams propagating in atmospheric turbulence" *Opt. Express*, **19**(27), 26444-50 (2011).
17. H. T. Eyyuboglu, C. Arpali, and Y. K. Baykal, "Flat topped beams and their characteristics in turbulent media," *Opt. Express* **14**(10), 4196–4207 (2006).
18. L. Allen, M. W. Beijersbergen, R. J. C. Spreeuw, and J. P. Woerdman, "Orbital angular momentum of light and the transformation of Laguerre–Gaussian laser modes," *Phys. Rev. A* **45**, 8185–8189 (1992).
19. S. Singh and A. K. Mishra, "Propagation Dynamics of Ultrashort Laguerre-Gauss Vortices in a Nonlinear Medium," 2022 Workshop on Recent Advances in Photonics (WRAP), 2022, pp. 1-2, doi: 10.1109/WRAP54064.2022.9758292.
20. S. Singh and A. K. Mishra, "Spatio-temporal evolution dynamics of ultrashort Laguerre–Gauss vortices in a dispersive and nonlinear medium," Accepted in *J. Opt.* <https://doi.org/10.1088/2040-8986/ac6df4>
21. O. Korotkova, L. C. Andrews, and R. L. Phillips, "Model for a partially coherent Gaussian beam in atmospheric turbulence with application in Lasercom," *Opt. Eng.* **43**(2), 330–341 (2004).
22. J. C. Ricklin and F. M. Davidson, "Atmospheric turbulence effects on a partially coherent Gaussian beam: implications for free-space laser communication," *J. Opt. Soc. Am. A* **19**(9), 1794–1802 (2002).
23. Y. Baykal, H. T. Eyyuboglu, and Y. Cai, "Scintillations of partially coherent multiple Gaussian beams in turbulence," *Applied Optics* **48**(10), 1943-1954 (2009).
24. Y. Gu, O. Korotkova, and G. Gbur, "Scintillation of nonuniformly polarized beams in atmospheric turbulence," *Opt. Lett.* **34**(15), 2261–2263 (2009)
25. J. Zhang, S. Ding, and A. Dang, "Polarization property changes of optical beam transmission in atmospheric turbulent channels," *Appl. Opt.* **56**(18), 5145–5155 (2017).
26. C. Wei, D. Wu, C. Liang, F. Wang, and Y. Cai, "Experimental verification of significant reduction of turbulence-induced scintillation in a full Poincare beam," *Opt. Express* **23**(19), 24331–24341 (2015)
27. F. Wang, X. Liu, L. Liu, Y. Yuan, and Y. Cai, "Experimental study of the scintillation index of a radially polarized beam with controllable spatial coherence," *Appl. Phys. Lett.* **103**(9), 091102 (2013)
28. Y. Gu and G. Gbur, "Scintillation of Airy beam arrays in atmospheric turbulence," *Opt. Lett.* **35**(20) (2010)
29. X. Ji and X. Li, "Directionality of Gaussian array beams propagating in atmospheric turbulence," *J. Opt. Soc. Am. A* **26**(2), 236-243 (2009)

30. T. Doster and A. T. Watnik, "Laguerre–Gauss and Bessel–Gauss beams propagation through turbulence: analysis of channel efficiency," *Appl. Opt.* **55**(36), 10239–10246 (2016)
31. M. Ghalaii and S. Pirandola, "Quantum communications in a moderate-to-strong turbulent space," *Commun. Phys.* **5**(38), (2022)
32. A. K. Jha, G. A. Tyler, and R. W. Boyd, "Effects of atmospheric turbulence on the entanglement of spatial two-qubit states," *Phys. Rev. A.* **81**(5), 053832–4 (2010)
33. X. Y. Chen, D. M. Deng, J. L. Zhuang, X. Peng, D. D. Li, L. P. Zhang, F. Zhao, X. B. Yang, H. Z. Liu, and G. H. Wang, "Focusing properties of circle Pearcey beams," *Opt. Lett.* **43**(15), 3626–3629 (2018).
34. X. Y. Chen, D. M. Deng, G. H. Wang, X. B. Yang, and H. Z. Liu, "Abruptly autofocused and rotated circular chirp Pearcey Gaussian vortex beams," *Opt. Lett.* **44**(4), 955–958 (2019).
35. C. Sun, D. M. Deng, X. B. Yang, and G. H. Wang, "Propagation dynamics of autofocusing circle Pearcey Gaussian vortex beams in a harmonic potential," *Opt. Express* **28**(1), 325–333 (2020).
36. L.Y. Zhu et.al., "Experimental demonstration and investigation of vortex circular Pearcey beams in a dynamically shaped fashion," *Opt. Express* **29**(13) 19819–30 (2021)
37. J. M. Martin, and S. M. Flatté, "Intensity images and statistics from numerical simulation of wave propagation in 3-D random media," *Appl. Opt.* **27**(11), 2111–2126 (1988).
38. J. M. Martin, and S. M. Flatté, "Simulation of point-source scintillation through three-dimensional random media," *J. Opt. Soc. Am. A* **7**(5), 838–847 (1990).
- 39 K. Khare, P. Lochab and P. Senthilkumaran, "Orbital Angular Momentum States of Light Propagation through atmospheric turbulence" IOP Publishing 2020